

Fiber Hybrid Polyimide-Based Composites Reinforced With Carbon Fiber and Poly-*p*-Phenylene Benzobisthiazole Fiber: Tribological Behaviors Under Sea Water Lubrication

Beibei Chen,¹ Jin Yang,¹ Jianzhang Wang,² Ning Liu,² Hongping Li,¹ Fengyuan Yan²

¹*Institute for Advanced Materials, School of Materials Science and Engineering, Jiangsu University, Zhenjiang 212013, China*

²*State Key Laboratory of Solid Lubrication, Lanzhou Institute of Chemical Physics, Chinese Academy of Sciences, Lanzhou 730000, China*

Fiber hybrid polyimide-based (PI-based) composites reinforced with carbon fiber (CF) and poly-*p*-phenylene benzobisthiazole (PBO) fiber of different volume fractions were fabricated by means of hot press molding technique, and their mechanical properties and tribological behaviors under sea water lubrication were systematically investigated in relation to the synergism of CF and PBO fiber. Results showed that the incorporation of CF or PBO fiber improved the tensile strength, hardness, and wear resistance of PI. More importantly, because of the synergistic enhancement effect between CF and PBO fiber on PI matrix, the combination of 10%CF and 5%PBO fiber reinforced PI-based composite had the best mechanical and tribological properties, showing promising application in ocean environment. POLYM. COMPOS., 37:1650–1658, 2016. © 2014 Society of Plastics Engineers

INTRODUCTION

Many mechanical components of devices used in marine environment, that is, pump, trail shaft, hydraulic drive system and so forth, are prone to wear and corro-

sion during their operating process, which requires these components to have outstanding properties of antiwear and corrosion resistance. Therefore, designing and developing high performance tribomaterials with the integration of excellent tribological properties and corrosion resistance is significant [1, 2].

Fiber reinforced polymer-based composites are the most rapidly growing class of materials, due to the good combination of low density, high specific strength and specific modulus, excellent antiwear and corrosion resistance [3–7]. And fiber hybrid polymer-based composites reinforced with two or more kinds of fibers not only possess the advantages of the composites reinforced with single kind of fiber, but also exhibit unique qualities, so they have been paid great attention and already widely used in the aerospace, military, industry, and other advanced fields [8–15]. In particular, fiber hybrid polymer-based composites have been accepted as self-lubricant materials and used in driving components/systems supposed to run without any external lubricants [11, 12, 14]. Accordingly, fiber hybrid polymer-based composites are promising tribomaterials suitable for ocean environment.

Polyimide (PI), a famous engineering plastic, has linear or cyclic imide units and aromatic groups providing many extraordinary characteristics, that is, high mechanical strength, good thermal stability, good resistance to oil, dilute acid, or low concentration alkali solution., superior corrosion resistance, and so forth. Nevertheless, long run-in stage, high friction coefficient and poor wear resistance of neat PI greatly limit its application in the field of tribology [16, 17]. So many previous researchers have made great efforts to improve its friction-reducing and wear resistant properties by means of filling different fillers [18–20]. Carbon fiber (CF) with high specific strength, specific modulus, high thermal conductivity, and good

Correspondence to: B. Chen; e-mail: chenbb@ujs.edu.cn

Contract grant sponsor: National Nature Science Foundation of China; contract grant number: 51405199 and 51372103; contract grant sponsor: Natural Science Foundation of Jiangsu Province; contract grant number: BK20140551, BK20140562; contract grant sponsor: Postdoctoral Science Foundation of China; contract grant number: 2014M561579; contract grant sponsor: Postdoctoral Science Foundation of Jiangsu Province; contract grant number: 1401106C; contract grant sponsor: Opening Foundation of Jiangsu Province Material Tribology Key Laboratory; contract grant number: Kjsmex201304; contract grant sponsor: Senior Intellectuals Fund of Jiangsu University; contract grant number: 13JDG099.

DOI 10.1002/pc.23337

Published online in Wiley Online Library (wileyonlinelibrary.com).

© 2014 Society of Plastics Engineers

TABLE 1. Mechanical properties of CF and PBO fiber.

Fiber	Modulus of elasticity (GPa)	Tensile strength (GPa)	Compressive strength (GPa)	Elongation (%)
PBO fiber	270	5.8	0.561	2.5
CF	250	2.5	0.8	1.5

self-lubricant property, is widely used in polymer matrix as reinforcement to fabricate high performance polymer-based composites. However, the disadvantages of low elongation and poor fracture toughness of CF always lead to relatively poor wear resistance of the corresponding composites under harsh sliding conditions [21]. While poly(*p*-phenylene benzobisoxazole) fiber (PBO fiber), a rigid-rod isotropic crystal polymer material, not only can be used as reinforcement for advanced composites, but also can compensate for the disadvantages of CF due to its high Young modulus, superior tensile strength and fracture elongation and so forth (Table 1 gives the mechanical properties of CF and PBO fiber). Therefore, the hybrid incorporation of CF and PBO fiber is a promising method to improve the comprehensive properties of polymer matrix. Regrettably, current investigations on the fiber hybrid are most focused on CF and glass fiber [22], CF and aramid fiber [23, 24], CF and ceramic/metallic fiber etc. [25–27], scarcely on the CF and PBO fiber.

In this study, fiber hybrid PI-based composites reinforced with various contents of CF and PBO fiber were prepared by hot press molding technique, and their tribological behaviors under sea water lubrication were investigated systematically. In addition, the tensile strength and Shore hardness of PI-based composites have been tested (the reported hardness is Shore D hardness which is mainly used to characterize the hardness of hard plastic). Moreover, the synergistic mechanisms between CF and PBO fiber enhancing the tribological properties of PI were discussed in detail. Hopefully, this research is to provide some guidance for designing and fabricating PI-based composites with excellent wear resistance under marine environment.

EXPERIMENTAL

Materials

Thermoplastic PI (YS-20) powder (particle size of < 75 μm , density of 1.38 g/cm^3) was commercially obtained from Shanghai Synthetic Resin Institute (China). CF (HT, average diameter of 7 μm , length of 28–56 μm , density of 1.77 g/cm^3) was provided by Nanjing Fiberglass R&D Institute (China). And the CF is PAN-based precursor. Poly-*p*-phenylene benzobisthiazole (Zylon, PBO) fiber (average diameter: 12 μm , length of 1 mm, density of 1.56 g/cm^3) was purchased from Toyobo (Japan). Figure 1 and Table 1 exhibit the scanning electron microscope

(SEM) micrographs and mechanical properties of CF and PBO fiber, respectively.

Six kinds of fiber hybrid PI-based composites with CF and/or PBO fiber, including PI-15%CF, PI-12%CF-3%PBO, PI-10%CF-5%PBO, PI-8%CF-7%PBO, PI-5%CF-10%PBO, and PI-15%PBO (volume fraction; corresponding PI-based composites were denoted as PI-1, PI-2, PI-3, PI-4, PI-5, and PI-6, respectively) were prepared by means of hot press molding technique. Specifically, the powders of PI and fibers in the appropriate proportion were mixed mechanically. Then the mixtures were filled into a mould, and sintered following the steps below: the mould was first heated to 300°C at the rate of 6°C/min; then slowly heated to 347°C at the rate of 1°C/min; and kept at 347°C for 60 min. During the whole heating process, the pressure was kept at 30 MPa. After naturally cooled below 100°C and released from the mould, the PI-based composite were obtained. Then the as-prepared PI and its composites were cut into presizes for tribological and mechanical test.

316 stainless steel (composition: $\leq 0.08\%$ C, $\leq 1.00\%$ Si, $\leq 2.00\%$ Mn, $\leq 0.035\%$ P, $\leq 0.03\%$ S, 10.0%~14.0% Ni, 16.0%~18.5% Cr, 2.0%~3.0% Mo, and balance Fe, at weight fraction) was used as the counterpart material, and its Vickers-hardness was HV347.

In this study, sea water was prepared according to ASTM D1141-98 (2013) standard. The chemical composition of sea water is shown in Table 2, where the gross concentration employed in the standard is an average of many reliable individual analyses.

Characterization

The Shore D hardness of as-prepared PI and its composites was measured using Shore Durometer, and their tensile strength was determined in universal material testing machine (DY-35) (the specimens were dumbbell shape with 115 mm in length, 25 mm in width at the end, 6 mm in width at the narrow portion, and 2 mm in thickness). The reported hardness and tensile strength were the average of three repeat measurements.

The friction and wear properties of PI and its composites were evaluated using a block-on-ring test rig. The details about the test were described elsewhere [21]. Specially, the schematic contact diagram of the frictional couple is shown in Fig. 2. The upper block was polymer specimen, the lower ring with a size of $\phi 49.22 \text{ mm} \times 13.06 \text{ mm}$ was made of 316 stainless steel. During the friction and wear test, the upper polymer specimen is fixed, while the lower 316 stainless steel ring is rotating. In this study, sliding was performed with a period of 120 min, sliding speeds of 0.5 m/s (200 r/min) and 1 m/s (400 r/min), normal loads of 200N, 400N, and 600N. Before each test, the surfaces of steel ring and polymer blocks were abraded to reach a surface roughness of about Ra 0.1 μm , and then cleaned with acetone. A container is full of sea water, and it has a water outlet valve which

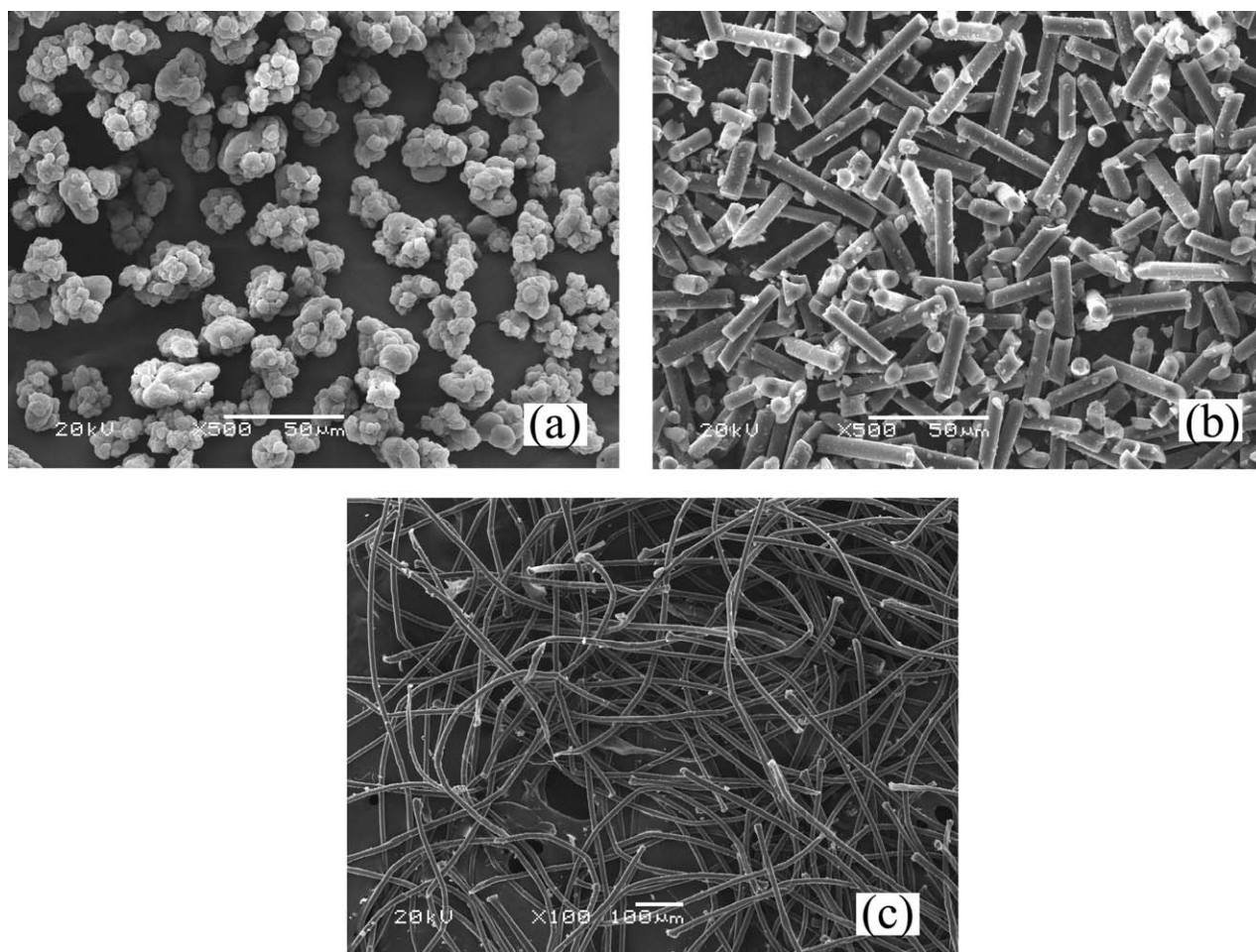


FIG. 1. SEM images of PI and fibers: (a) PI; (b) CF; and (c) PBO fiber.

can alter the rate of outflow. And we fix a plastic tube on the water outlet valve, and the other end of the tube reach the surface of 316 steel nearby. During the friction and wear test, the sea water is continuously dropping onto the sliding surface at a rate of 100–105 drops per minute (300–315 mL/h) which is controlled by altering the water outlet valve. Before the friction and wear test, a load has been applied on the polymer specimen, and then the counterpart starts to rotate. The applied load (F) and

friction force (f) are continuously recorded by an online data acquisition system attached to the tester until the friction and wear test has been finished. And the instantaneous friction coefficient at any time can be obtained through the computation module which is based on the formula:

TABLE 2. Chemical composition of sea water (chlorinity is 19.38, pH is 8.20).

Compound	Concentration (g/L)
NaCl	24.53
MgCl ₂	5.20
Na ₂ SO ₄	4.09
CaCl ₂	1.16
KCl	0.695
NaHCO ₃	0.201
KBr	0.101
H ₃ BO ₃	0.027
SrCl ₂	0.025
NaF	0.003

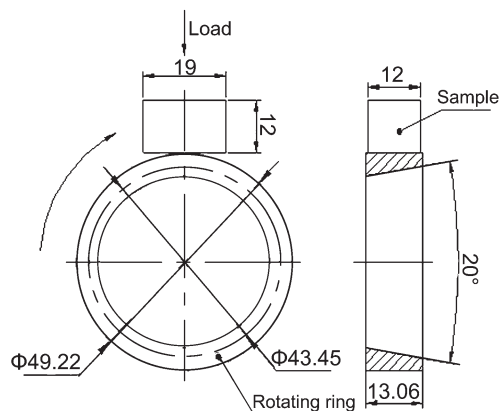


FIG. 2. Contact schematic diagram for the frictional couple (units: mm).

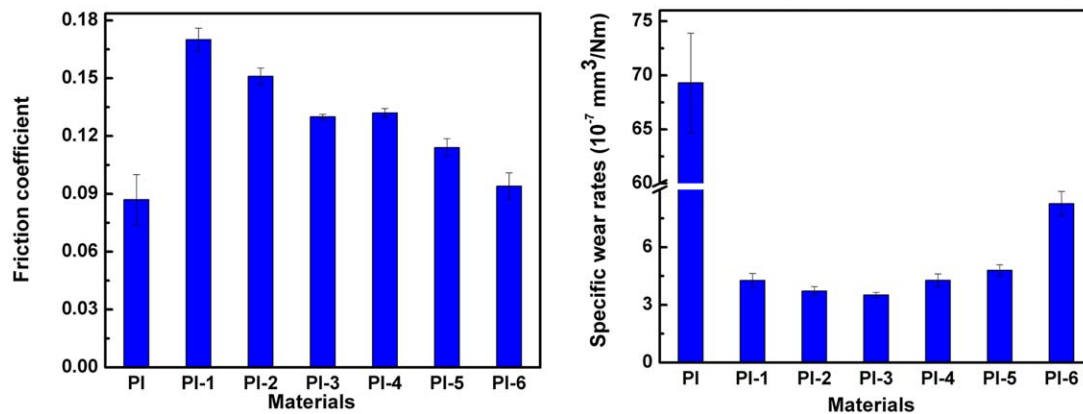


FIG. 3. Friction coefficients and wear rates of PI and its composites sliding against 316 steel under sea water lubrication (load: 200N, sliding speed: 0.5 m/s, duration: 120 min). [Color figure can be viewed in the online issue, which is available at wileyonlinelibrary.com.]

$$\mu = \frac{f}{F} \quad (1)$$

and the reported friction coefficient was the average value during the whole friction test. After the friction test, the width of the wear track on the specimen block was measured using an optical microscope (OM) with an accuracy of 0.01 mm. The specific wear rate (K) of the specimens was calculated from the relationships [28]:

$$V = B \left[R^2 \arcsin \frac{b}{2R} - \frac{b}{2} \sqrt{R^2 - \frac{b^2}{4}} \right] \quad (2)$$

$$K = \frac{V}{L \cdot d} \quad (3)$$

where V is the wear volume loss (mm^3), B is the width of the block sample (mm), R is the radius of the steel ring (mm), b is the width of the wear track (mm), d is the sliding distance (mm), and L is the load (N). Three repeated tests were carried out for each specimen, and the average of three repeated tests was reported.

The worn surfaces of PI and its composites were examined using a JEM-5600LV SEM. To increase the resolution for the SEM observation, the tested polymer samples were plated with gold coating to render them electrically conductive. In addition, OM was used to observe the details of fiber on the worn surfaces of PI-based composites as well.

RESULTS AND DISCUSSION

Friction and Wear Properties

Figure 3 exhibits the friction coefficients and wear rates of PI and its composites sliding against 316 steel under the lubrication of sea water. It can be clearly seen that the incorporation of CF and/or PBO fiber can hardly improve the friction-reducing property of PI, but greatly increase the wear resistance. In particular, the variation of friction

coefficient of PI and its composites with sliding time is shown in Fig. 4. It can be clearly seen that the friction coefficient of pure PI fluctuates dramatically during the whole friction and wear process, and its running-time is nearly 3000 s which is much longer than those of PI-based composites. Besides, although the friction coefficients of all PI-based composites are higher than that of pure PI, they have slight fluctuation with the sliding time increasing. Compared to PBO fiber, CF has much better reinforcement effect on the wear resistance of PI. Specially, the wear rate of PI-1 composite (PI-15%CF) is only half of that of PI-6 composite (PI-15%PBO). In addition, it can be found that the incorporation of PBO fiber to CF/PI composite further enhances its friction-reducing and wear-resistant properties under sea water lubrication. And the friction coefficient and wear rate of PI-CF-PBO composites decrease with the increase in PBO fiber content. It is worth noting that the wear rate of fiber hybrid PI-composite begins to increase, when the content of PBO fiber surpasses 5% or the content

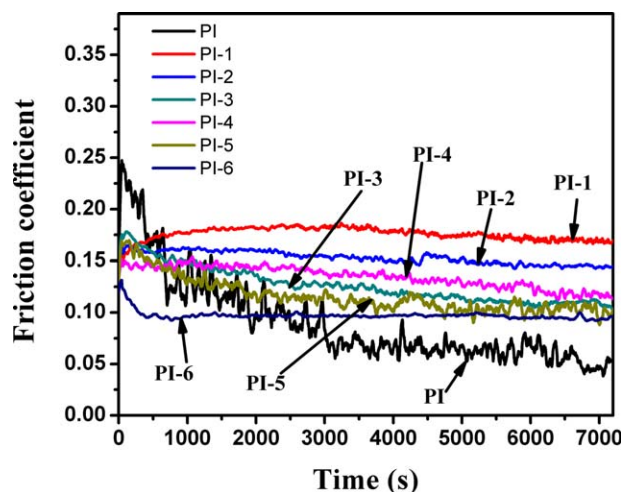


FIG. 4. Variation of friction coefficient of PI and its composites with sliding time in sea water (Load: 200N, sliding speed: 0.5 m/s, duration: 120 min). [Color figure can be viewed in the online issue, which is available at wileyonlinelibrary.com.]

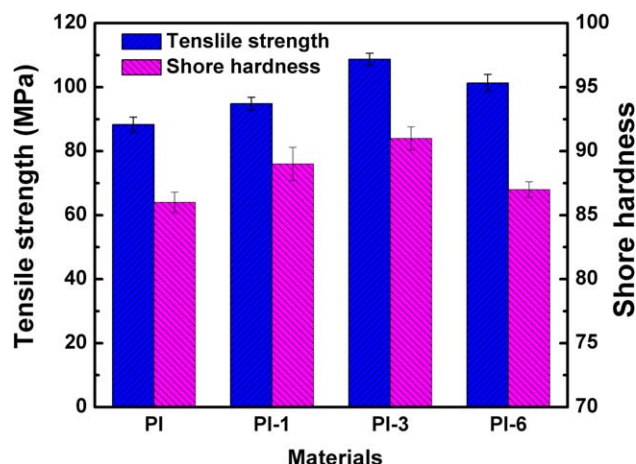


FIG. 5. Mechanical properties of PI and its composite. [Color figure can be viewed in the online issue, which is available at wileyonlinelibrary.com.]

of CF is below 10%. Therefore, the fiber hybrid PI-based composite reinforced with 5%PBO and 10%CF (PI-3 composite) possesses much better wear resistance not only than unfilled PI but also than PI reinforced with CF or PBO fiber alone. This suggests that there exists the synergistic enhancement effect on the wear resistance of PI matrix when the volume fractions of CF and PBO fiber are 10 and 5%, respectively. Generally, the friction and wear properties of polymer-based composites are closely related to their mechanical properties [16, 29]. To better understand the enhancement effect of CF and PBO fiber, Fig. 5 gives the mechanical properties of PI-based composites reinforced with CF and/or PBO fiber. It can be found that the incorporation of PBO fiber with super-high elastic modulus improves the tensile strength of PI, while CF with high compressive strength improves the hardness of PI obviously. That is, PBO fiber and CF can enhance the toughness and load-carrying capacity of PI, respectively. More importantly, the simultaneous incorporation of 5%PBO fiber and 10% CF reinforced PI-based composite (PI-3 composite) has higher tensile strength and hardness than PI-1 and PI-6. This might be the reason why PI-3 composite has excellent friction and wear properties compared to PI-based composites reinforced with single kind of fiber.

As an example of PI-3 composite (PI-10%CF-5%PBO), the variation of its friction coefficient and wear rate with load and sliding speed is shown in Fig. 6. It can be seen that the friction coefficient and wear rate of PI-3 composite increase with increasing load. And this result is on the contrary to some investigations about the tribological behaviors of polymer-based composites under dry friction [30, 31]. As is well known, sliding between materials always results in heat generation and hence increases the temperature of two frictional surfaces. And a high applied load always leads to a dramatic temperature increase at sliding surfaces under dry friction condition. Thus, the polymer surface might be softened, and this might be followed by a decrease in the shear strength, which facilitates the polymer materials to be sheared and further leads to low friction

coefficient. But in our present study, sea water as excellent cooling medium well facilitates the dissipation of the friction-induced heat and decreases the temperature of contact zones, which is favorable for PI-3 composite to retain a high shear strength. Moreover, the increase in load is favorable for increasing real contact area and further greatly decreases the degree of separation between the frictional pairs by sea water film, finally resulting in increased friction coefficient. Therefore, the friction coefficient of PI-3 composite sliding against 316 steel in sea water increases with increasing load. In addition, high load leads to accelerated pull-out, bending, and breakage of CF and/or PBO fiber in the PI-based composite. As a result, the load-carrying capacity of composite is decreased and the broken CF and/or PBO fiber act as abrasive particles to abrade the composite surface. Accordingly, the wear rate of PI-3 composite increases with the increase in load as well.

In addition, the tribological behaviors of PI-3 composite under sea water lubrication are influenced by the formation and maintenance of the sea water film between the two contact surfaces, which are greatly affected by the sliding conditions. According to the investigations of Yamamoto and Takashima [32], the degree of separation is determined by bearing modulus ϕ , $\phi = \eta N/P$ where η is the viscosity, N is the sliding speed, and P is the contact pressure. Therefore, the lower applied load or the higher sliding speed, the larger degree of separation of the frictional pairs by water film and hence less severe damage of the contact surfaces, finally leading to lowered friction coefficient and wear rate. This well explains why PI-3 composite has higher friction coefficient and wear rate under higher load, but better tribological properties under higher sliding speed.

SEM and OM Micrographs of Worn Surfaces of Fiber Hybrid PI-based Composites

Figure 7 shows the SEM images of worn surfaces PI and its composites sliding against 316 steel under sea

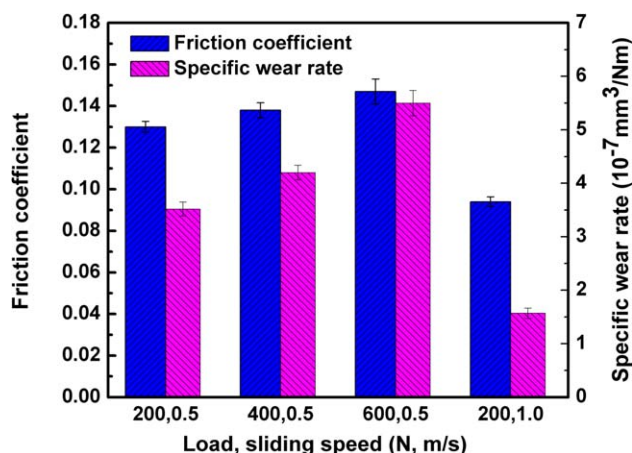


FIG. 6. Friction coefficients and wear rates of PI-10%CF-5%PBO composite sliding against 316 steel at different sliding conditions under sea water lubrication. [Color figure can be viewed in the online issue, which is available at wileyonlinelibrary.com.]

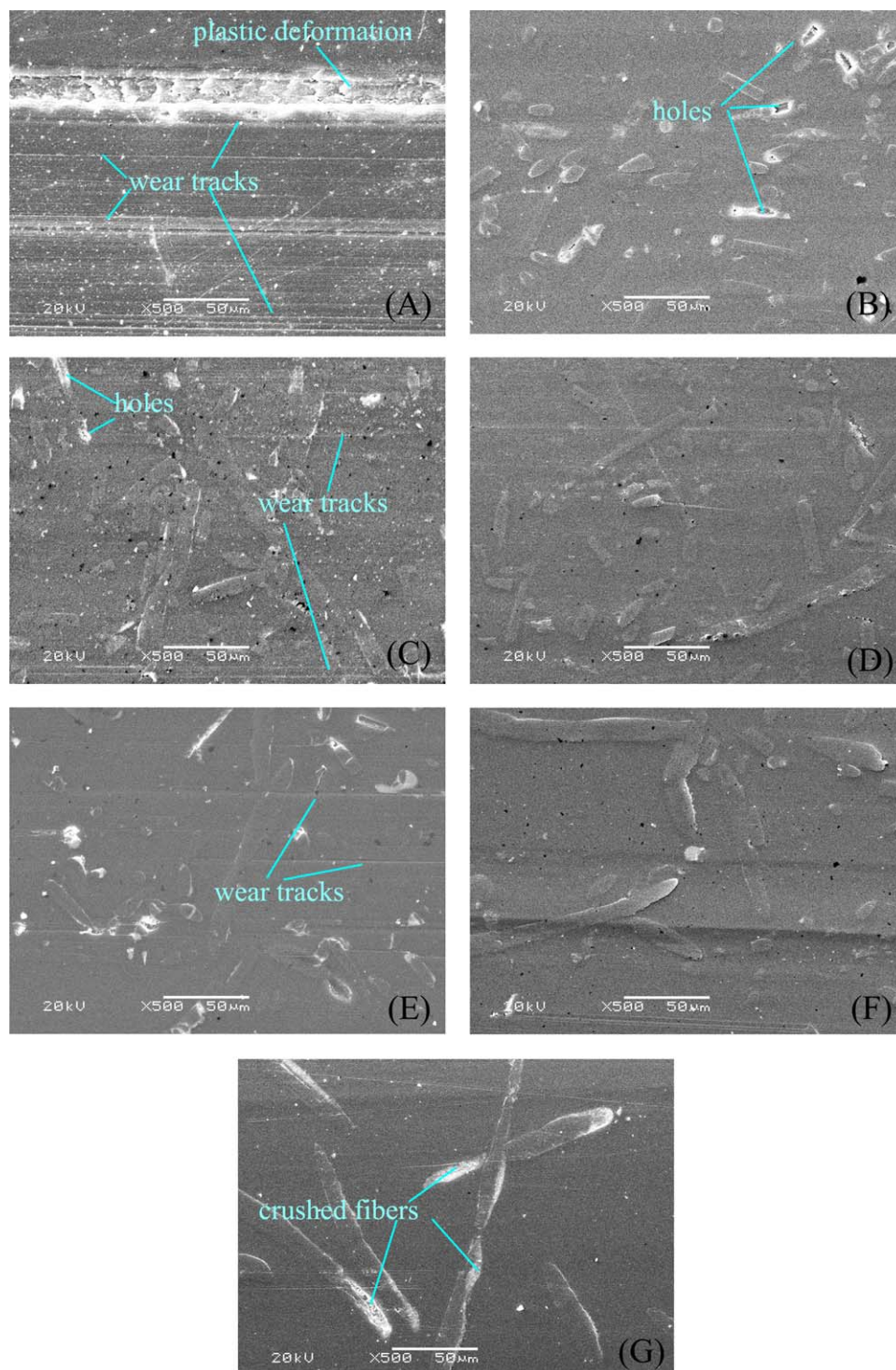


FIG. 7. SEM images of worn surfaces of PI and its composites sliding against 316 steel under sea water lubrication: (A) PI; (B) PI-1; (C) PI-2; (D) PI-3; (E) PI-4; (F) PI-5; and (G) PI-6 (Load: 200N, sliding speed: 0.5 m/s, duration: 120 min). [Color figure can be viewed in the online issue, which is available at wileyonlinelibrary.com.]

water lubrication at load of 200N and sliding speed of 0.5 m/s. The worn surface of pure PI is characterized by serious plastic deformation, wide and deep grooves (Fig. 7A), which implies that pure PI is dominated by severe abrasive wear during the friction and wear process. This

well corresponds to the poorest wear resistance of pure PI mentioned in Fig. 3. On the contrary, due to the reinforcement effect of CF and PBO fiber, there are scarcely obvious signs of plastic deformation and grooves on the worn surfaces of PI-based composites, with the exception

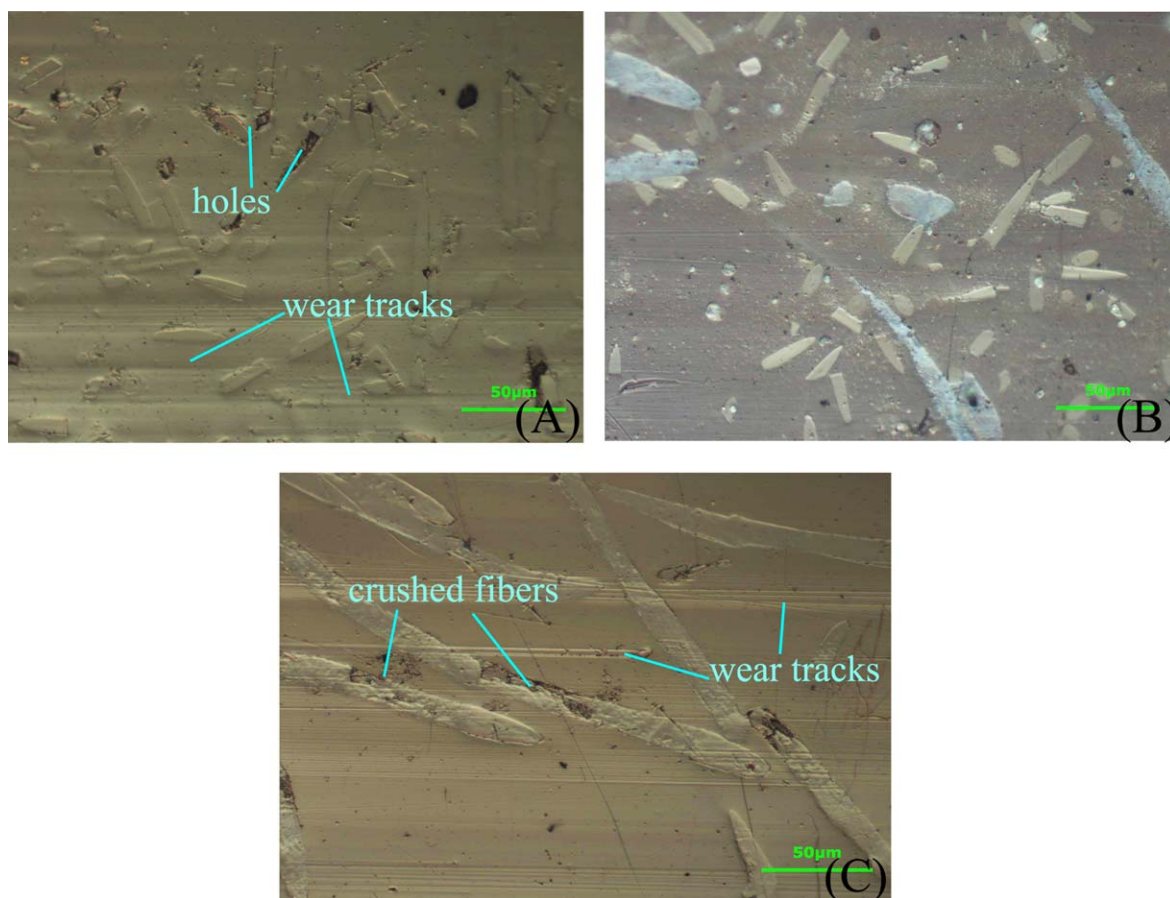


FIG. 8. OM images of worn surfaces of PI-based composites: (A) PI-1; (B) PI-3; and (C) PI-6. [Color figure can be viewed in the online issue, which is available at wileyonlinelibrary.com.]

of fine scratches. This not only well explains how the incorporation of CF and/or PBO fiber greatly improve the wear resistance of PI, but also suggests that the main wear mechanism for PI-based composites under sea water lubrication is slight abrasive wear. Nevertheless, the detailed characteristics of the worn surfaces of various PI-based composites are different. Specifically, the worn surface of PI-1 composite is barely with grooves, but there still exists some holes due to the pulling-out of CF from the PI matrix (Fig. 7B). However, the incorporation of PBO fiber greatly inhibits the pulling-out of CF from PI matrix, thus the corresponding worn surfaces of PI-CF-PBO composites scarcely exhibit the signs of CF being broken or pulled out (Fig. 7C–F). And with the PBO fiber content increasing, the worn surfaces become much smoother. Especially for PI-3 composite, its worn surface is the smoothest compared to those of other PI-based composites (Fig. 7D), which agrees well with PI-3 composite possessing the best wear resistance among all the PI-based composites. And when the PBO fiber content exceeds 5%, the worn surfaces of PI-CF-PBO composites become rougher than that of PI-3 composite due to the decreased reinforcement effect which is caused by the reduction of CF content. In particular, on the worn

surface of PI-based composite reinforced with the single kind PBO fiber (PI-6), there are some PBO fibers being bent, and even pulled out as a result of PBO fiber with low compressive strength carrying too much applied load, which accounts for its higher wear rate than those of PI-based composites reinforced with the combination of PBO fiber and CF in Fig. 3. In a word, the description above indicates that the 10%CF and 5%PBO has the best synergistic enhancement effect on the wear-resistant property of PI matrix.

To deeply discuss the synergistic enhancement effect between CF and PBO fiber on the tribological properties of PI, the specific details of worn surfaces of fiber hybrid PI-based composites have been investigated emphatically by OM observation. And Fig. 8 gives the OM images of worn surfaces of PI-1, PI-3, and PI-6. It can be found that either CF or PBO fiber on the worn surface of all PI-based composites is thinned. Besides, there are some holes on the worn surface of PI-1 as the result of the pulled-out CF, and there are obvious signs of PBO fiber being crushed or broken, while the worn surface of PI-3 is smooth and without any signs of fiber in failure. According to some previous studies [33, 34], short fiber can effectively improve the wear resistance of polymer-

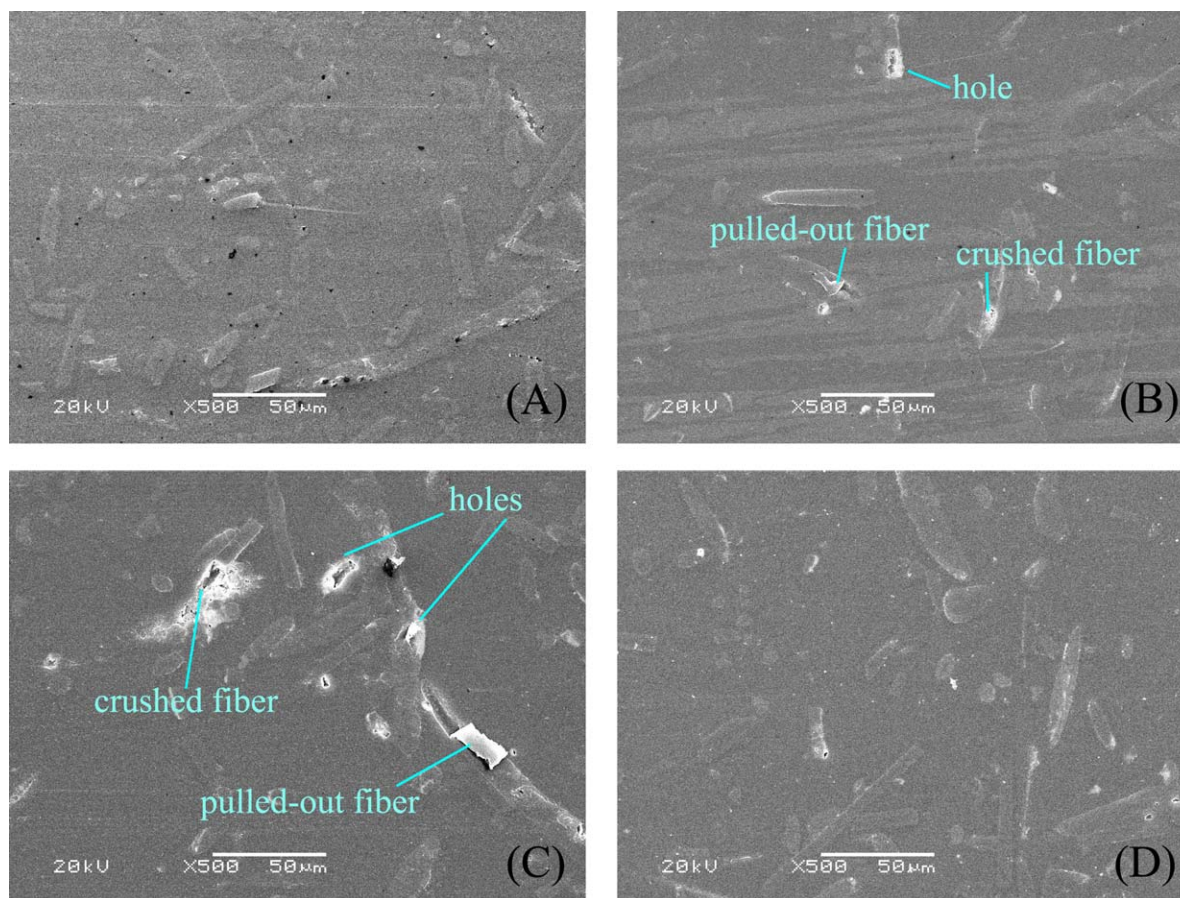


FIG. 9. SEM images of worn surfaces of PI-3 composite sliding against 316 steel at different sliding conditions under sea water lubrication: (A) 200N, 0.5 m/s; (B) 400N, 0.5 m/s; (C) 600N, 0.5 m/s; and (D) 200N, 1.0 m/s. [Color figure can be viewed in the online issue, which is available at wileyonlinelibrary.com.]

based composites by undergoing most of applied load during sliding process. And the process mainly includes: (1) matrix wear, (2) fiber thinning, (3) fiber broken, and (4) fiber peeling-off. In this study, PI matrix with poor wear resistance is firstly worn off during the friction and wear process, and CF and/or PBO fiber are exposed on the worn surfaces acting as the strong barriers against plowing effect of counterpart asperities, so the friction coefficients of fiber hybrid PI-based composites are much higher compared to that of pure PI. And just for this, the exposed CF and/or PBO fiber effectively protect PI matrix from being worn off by carrying the most of applied load on the sliding surfaces. Because CF with higher compressive strength than PBO fiber can resist the plowing effect of asperities of 316 steel effectively, there are scarcely grooves on the worn surface of PI-1 composite. But brittle CF carries so much applied load on the sliding surfaces that it is easily to be broken and pulled out from PI-1 composite leaving some holes (Fig. 8A). This decreases the load-carrying capacity of PI-1 composite and further deteriorates its tribological properties. For PI-6 composite, PBO fiber with low compressive strength cannot be sufficient to carry the applied load and resist the

plowing effect of the counterpart, thus the worn surface is rough with many grooves (Fig. 8C). This well explains why the wear resistance of PI-6 is inferior to that of PI-1 composite. However, PBO fiber is not easily being crushed under the applied load during the sliding process due to the excellent toughness, so any signs of holes of PBO fiber being pulled out can be scarcely seen on the worn surface of PI-6 composite. Because of outstanding properties of CF and PBO fiber, the low elongation and poor fracture toughness of CF can be compensated by PBO fiber, while the low compressive strength of PBO fiber can be made good by the incorporation of CF. That is, the simultaneous incorporation of CF and PBO fiber at a proper volume fraction can play the different roles in enhancing the comprehensive properties of PI matrix to a large extent. Meanwhile, PBO fiber with high toughness and CF with high compressive strength can share applied load on the sliding surface together to avoid any single kind of fiber being crushed or broken as a result of carrying too much applied load. Therefore, the combination of CF and PBO fiber reinforced PI-based composite (PI-3) has excellent tribological properties, even under the harsh sliding conditions of heavy load or high sliding speed.

In addition, Fig. 9 exhibits the worn surface of PI-3 composite sliding against 316 steel at different sliding conditions under sea water lubrication. It can be seen that the worn surface of PI-3 composite under high load is rougher than that under low load. Especially at 600N, there are many CFs and PBO fibers pulled out on the worn surface, and some even are bent or crushed (Fig. 9C), which not only greatly decrease the load-carrying capacity of PI-3 composite, but also lead to severe abrasive wear during sliding process. This is well consistent with larger wear rate and friction coefficient of PI-3 composite at higher load. Besides, the worn surface of PI-3 composite at 1.0 m/s is much smoother than that at 0.5 m/s because the higher sliding speed favors the formation and retaining of sea water film which can avoid to the direct contact of the counterparts.

CONCLUSIONS

1. Due to the synergistic enhancement effect of CF and PBO fiber, the mechanical and tribological properties of PI in sea water have been improved significantly.
2. The PI-based composite reinforced with 5%PBO fiber and 10%CF (PI-3 composite) has the best wear resistance, showing promising application in ocean environment.
3. The synergistic enhancement mechanism of CF and PBO fiber on PI matrix is that the disadvantages of low elongation and poor fracture toughness of CF can be compensated by PBO fiber, while the shortcoming of low load-carrying capacity of PBO fiber can be made good by the incorporation of CF. Meanwhile, during the friction and wear process, PBO fiber and CF can simultaneously share applied load on the sliding surface to avoid any single kind of fiber being broken as a result of carrying too much applied load.

REFERENCES

1. I. Serre, N. Celati, and R.M. Pradeilles-Duval, *Wear*, **252**, 711 (2002).
2. Z.Q. Wang and D.R. Gao, *Mater. Design*, **53**, 881 (2014).
3. J. Li and Y.C. Xia, *Polym. Compos.*, **31**, 536 (2010).
4. M. Sumer, H. Unal, and A. Mimaroglu, *Wear*, **265**, 1061 (2008).
5. T.M. Wang, G. Zhao, and Q.H. Wang, *Polym. Compos.*, **33**, 812 (2012).
6. F. Guo, Z.Z. Zhang, H.J. Zhang, and W.M. Liu, *Compos. A*, **40**, 1305 (2009).
7. J. Li and X.H. Cheng, *Polym. Compos.*, **30**, 59 (2009).
8. C.S. Dong, H.A. Ranaweera-Jayawardena, and I.J. Davies, *Compos. B*, **43**(2), 573 (2012).
9. Q. Chen, Y. Zhao, Z.P. Zhou, A. Rahman, X.F. Wu, W.D. Wu, T. Xu, and H. Fong, *Compos. B*, **44**(1), 1 (2013).
10. K. John and S.V. Naidu, *J. Reinf. Plast. Comp.*, **23**(12), 1253 (2004).

11. M. Boopalan, M. Niranjanaa, and M.J. Umapathy, *Compos. Part B-Eng.*, **51**, 54 (2013).
12. T. Tsukizoe and N. Ohmae, "Friction and Wear Performance of Unidirectionally Oriented Glass, Carbon, Aramid and Stainless Steel Fiber-Reinforced Plastics," in *Friction and Wear of Polymer Composites*, Amsterdam, Elsevier, 205 (1986).
13. I.D.G. Ary Subagia, Y. Kim, L.D. Tijing, C.S. Kim, and H.K. Shon, *Compos. Part B-Eng.*, **58**, 251 (2014).
14. F.H. Su, Z.Z. Zhang, F. Guo, X.H. Men, and W.M. Liu, *Compos. Sci. Technol.*, **67**(6), 981 (2007).
15. S.Y. Fu, B. Lauke, E. Mäder, C.Y. Yue, X. Hu, and Y.W. Mai, *J. Mater. Sci.*, **36**(5), 1243 (2001).
16. H. Cai, F.Y. Yan, and Q.J. Xue, *Mat. Sci. Eng. A-Struct.*, **364**, 94 (2004).
17. Y.J. Shi, L.W. Mu, X. Feng, and X.H. Lu, *J. Appl. Polym. Sci.*, **121**, 1574 (2011).
18. A. Tanaka, K. Umeda, M. Yudasaka, M. Suzuki, T. Ohana, M. Yumura, and S. Iijima, *Tribol. Lett.*, **19**(2), 135 (2005).
19. S. Pieter, D.B. Patrick, and S. Gustaaf, *J. Appl. Polym. Sci.*, **116**, 1146 (2010).
20. J. Li and X.H. Cheng, *Mater. Chem. Phys.*, **108**, 67 (2008).
21. B.B. Chen, J.Z. Wang, and F.Y. Yan, *Tribol. Int.*, **52**, 170 (2012).
22. K. Friedrich and O. Jacobs, *Compos. Sci. Technol.*, **43**, 71 (1992).
23. J. Gustin, A. Joneson, M. Mahinfalah, and J. Stone, *Compos. Struct.*, **69**, 396 (2005).
24. Y.Z. Wan, Y. Huang, F. He, Q.Y. Li, and J.J. Lian, *Mat. Sci. Eng. A-Struct.*, **452**, 202 (2007).
25. M. Kumar, B.K. Satapathy, A. Patnaik, D.K. Kolluri, and B.S. Tomar, *Tribol. Int.*, **44**(4), 359 (2011).
26. A. Patnaik, M. Kumar, B.K. Satapathy, and B.S. Tomar, *Wear*, **269**, 891 (2010).
27. H. Fu, B. Liao, F.J. Qi, B.C. Sun, A.P. Liu, and D.L. Ren, *Compos. B* **39**(4), 585 (2008).
28. ASTM G77-05, Standard Test Method for Ranking Resistance of Materials to Sliding Wear Using Block-on-Ring Wear Test, American Society for Testing and Materials (2010).
29. D.S. Xiong, *Mater. Lett.*, **59**(2–3), 175 (2005).
30. Q.H. Wang, X.R. Zhang, and X.Q. Pei, *Mater. Design*, **31**(8), 3761 (2010).
31. X.R. Zhang, X.Q. Pei, and Q.H. Wang, *Mater. Design*, **30**(10), 4414 (2009).
32. Y. Yamamoto and T. Takashima, *Wear*, **253**(7–8), 820 (2002).
33. G.Y. Xie, G.X. Sui, and R. Yang, *Compos. Sci. Technol.*, **71**(6), 828 (2011).
34. L. Chang and K. Friedrich, *Tribol. Int.*, **43**(12), 2355 (2010).